Available online at www.sciencedirect.com
ScienceDirect
Journal of Non-Crystalline Solids 353 (2007) 3154–3159
JOURNAL OF NON-CRYSTALLINE SOLIDS
www.elsevier.com/locate/jnoncrysol

High frequency collective dynamics in liquid potassium

A. Monaco [a,*], T. Scopigno [b], P. Benassi [c], A. Giugni [c], G. Monaco [a], M. Nardone [c], G. Ruocco [b], M. Sampoli [d]

[a] European Synchrotron Radiation Facility, B.P. 220 F-38043 Grenoble cedex, France
[b] Dipartimento di Fisica and INFM, Universita' di Roma "La Sapienza", I-00185, Roma, Italy
[c] Dipartimento di Fisica and INFM, Universita' di L'Aquila, I-67010, L'Aquila, Italy
[d] Dipartimento di Energetica and INFM, Universita' di Firenze, I-50019, Firenze, Italy

Available online 16 July 2007

Abstract

We investigated by inelastic X-ray scattering the dynamical properties of molten potassium in a wide range of momentum transfer, Q, from 1 nm^{-1} up to the main peak of the structure factor $Q \approx 17\ nm^{-1}$. The observed increase of sound velocity in the low Q region ($1 < Q < 3\ nm^{-1}$), has been described within a model characterized by two distinct relaxation processes for the collective dynamics. The obtained results are discussed and compared with those from previous neutron scattering experiments. In particular, we associate the speed-up of the sound velocity to the 'instantaneous' disorder of the liquid as opposed to the argument, supported by some neutron scattering studies, of a transition from a liquid to solid like response of the system.
© 2007 Elsevier B.V. All rights reserved.

PACS: 61.20.Lc

Keywords: Acoustic properties and phonons; Liquid alloys and liquid metals; Diffraction and scattering measurements; Modeling and simulation; Structure; X-rays

1. Introduction

The study of the microscopic dynamics of simple liquids received in the last few years has renewed interest, particularly from the point of view of experimental investigations [1–10]. In fact, thanks to the parallel application of similar spectroscopic techniques, namely inelastic X-ray scattering (IXS) and inelastic neutron scattering (INS), it is possible today to go deeper into the investigation of the microscopic mechanisms controlling the dynamical behavior of a simple liquid, being well supported by experimental results.

In particular, one of the preferred classes of systems, selected to study collective and single particle dynamics, is represented by the alkali metals. These liquids, indeed, present well-pronounced inelastic features in their density fluctuation frequency spectra, even at length-scales far away from the hydrodynamic limit and comparable with the average distance between the particles.

Looking at collective properties, IXS spectroscopy technique has been massively adopted in the recent past [1,7–9] in order to get an insight into the ultimate mechanisms ruling the high frequency dynamics. In the present study we report an investigation of the dynamics of liquid potassium in a wide wave vector–energy (Q–E) region. We discuss possible models to describe the collective dynamics through a comparison with similar INS data recently published [3,4].

More specifically, several recent experimental investigations of liquid dynamics have put forward the crucial role played by the memory function formalism [1,5,6,9,10], a framework tailored to account for the relaxation spectra of the density fluctuations over an extended wave-length energy range. Most of the work of the present study on liquid potassium has been devoted to understand how the evolution of the $S(Q,\omega)$, varying Q values, could be described with a suitable memory function model.

* Corresponding author. Tel.: +39 3391096035; fax: +39 0862689713.
E-mail address: andreamona@gmail.com (A. Monaco).

0022-3093/$ - see front matter © 2007 Elsevier B.V. All rights reserved.
doi:10.1016/j.jnoncrysol.2007.05.049

On a theoretical ground, the hydrodynamic equation of a simple fluid predicts the presence of two distinct relaxation processes for the decay of the density fluctuations [10,11], one associated with the coupling of density and temperature fluctuations and another stemming from the viscous relaxation.

Starting from these indications on the nature of the relaxation processes in the hydrodynamic limit, we test the soundness of a model where the viscous relaxation proceed through two distinct channels [13–16] which are active on quite different time scales. This model, already applied in other systems [1,5,6,9,10], depicts a microscopic scenario where the atoms experience, in the sub-pico-seconds time region (τ_μ), the interaction with the surrounding neighbors. This relaxation process has been termed as microscopic and instantaneous, in contrast to the structural relaxation time that acts on a longer timescale and controls the rearrangement of the instantaneous atomic equilibrium configuration.

The purpose of the present paper has been first to observe the evolution of the dynamics of the liquid at different lengths, studying the dominant excitation frequency of the $S(Q,\omega)$. Then we proceed in the description of the microscopic mechanism of the liquid exploiting the physical meaning of the parameters involved in the model. Our attention has been focused on the low Q region where INS experiments are affected by well-known kinematics limitations.

Previous INS investigations of liquid potassium have been analyzed with both an empirical [3] and memory function framework [4], similar to the one adopted in previous IXS studies [1,5,6,9,10]. The values of speed of sound deduced from the INS experiments exceed the hydrodynamic value, and such phenomenon has been interpreted as reminiscence of the crystal like sound propagation. This explanation, which stems from an interpretation of the relaxation dynamics in terms of a liquid to solid like transition, is here discussed also in view of several other results reported in other liquids and (numerically) supercooled and glassy metals (Li, Na, Al, Ga) [1,5,6,9,10,17,18].

2. Experiment

We report here the determination, by means of the IXS spectroscopy, of the dynamic structure factor of liquid potassium in the Q range from 1 nm^{-1} to 16 nm^{-1}. The experiment has been performed at the high-resolution beam line ID16 at the European Synchrotron Radiation Facility, in a fixed exchanged wave-vector configuration. Thanks to the presence of a five analyzers bench, we collected simultaneously five different values of Q, then we have been able to map the planned Q range with a satisfying accuracy spending a reasonable time for the data acquisition. For all spectra, we performed an energy scan (−50 to 50 meV) that took about 300 min and was repeated to collect 300 s per point of total integration time. During the measurements we fixed the temperature of the potassium slightly above the melting point at $T = 343 \pm 1$ K, keeping the sample under vacuum. The sample holder for liquid potassium was made out of two pieces of austenitic steel which was able to conform the liquid to be confined with a thickness of 1 mm. Such length corresponds to the absorption length of the potassium at the energy of the incident beam. The energy resolution used during the measurements, 1.5 meV (FWHM), corresponds to the chosen reflection of the silicon analyzer (11 11 11) for an incident energy of the beam of 21 748 eV. In Fig. 1, we show the collected raw spectra in all the explored Q range. It is evident, even at this level, the presence of a dispersion behavior of the inelastic structure of the spectra; the dispersion reaches the maximum at $Q = 10$ nm^{-1} and progressively decreases when Q approaches the main peak of the static structure factor 16 nm^{-1}.

3. Analysis and discussion

In order to quantify the role of the different microscopic mechanisms that drive the dynamics of liquid potassium, we modelled the dynamical $S(Q,\omega)$ using the memory function formalism. Starting from the generalized Langevin equation, is possible to write $S(Q,\omega)$ in terms of real ($M'(Q,t)$) and imaginary ($M''(Q,t)$) part of the Fourier–Laplace transform function $M(Q,t)$ [11,12], so that

$$S(Q,\omega) = \frac{S(Q)\pi^{-1}\omega_0^2(Q)M'(Q,\omega)}{[\omega^2 - \omega_0^2(Q) + \omega M''(Q,\omega)]^2 + [\omega M'(Q,\omega)]^2}.$$

Here we have introduced the frequency $\omega_0(Q) = KTQ^2/\mathrm{mS(Q)}$ calculated from the liquid static structure factor $S(Q)$, this quantity is directly connected to the generalized isothermal speed of sound through the relationship: $c_t(Q) = \omega_0(Q)/Q$.

The ultimate goal is, of course, to find the most appropriate shape for the $M(Q,t)$, each relaxation process entering the spectrum of the density fluctuation can be taken into account as an additive contribution to the second order memory function.

Starting from the generalization of the hydrodynamic we chose to use a model for the $S(Q,\omega)$ characterized by three distinct channels for the relaxation processes. The first channel arises from the coupling between the density and the temperature fluctuations, while the other two are associated with the viscous relaxation process.

$$M(Q,\omega) = (\gamma - 1)\omega_0^2(Q)e^{-D_T Q^2 t} + \Delta_\alpha^2(Q)e^{-t/\tau_\alpha(Q)} + \Delta_\mu^2(Q)e^{-t/\tau_\mu(Q)}.$$

The specific heat ratio γ and the thermal diffusivity D_T have been deduced from macroscopic data [19].

We use for the thermal contribution to the $M(Q,t)$ the generalized hydrodynamic result, i.e. the usual Debye expression, known as viscoelastic model [20], neglecting any Q dependence of the diffusion coefficient. Moreover, similarly to previous studies on alkali metals [1,5,6,9,10,18], we adopt a two exponential functions

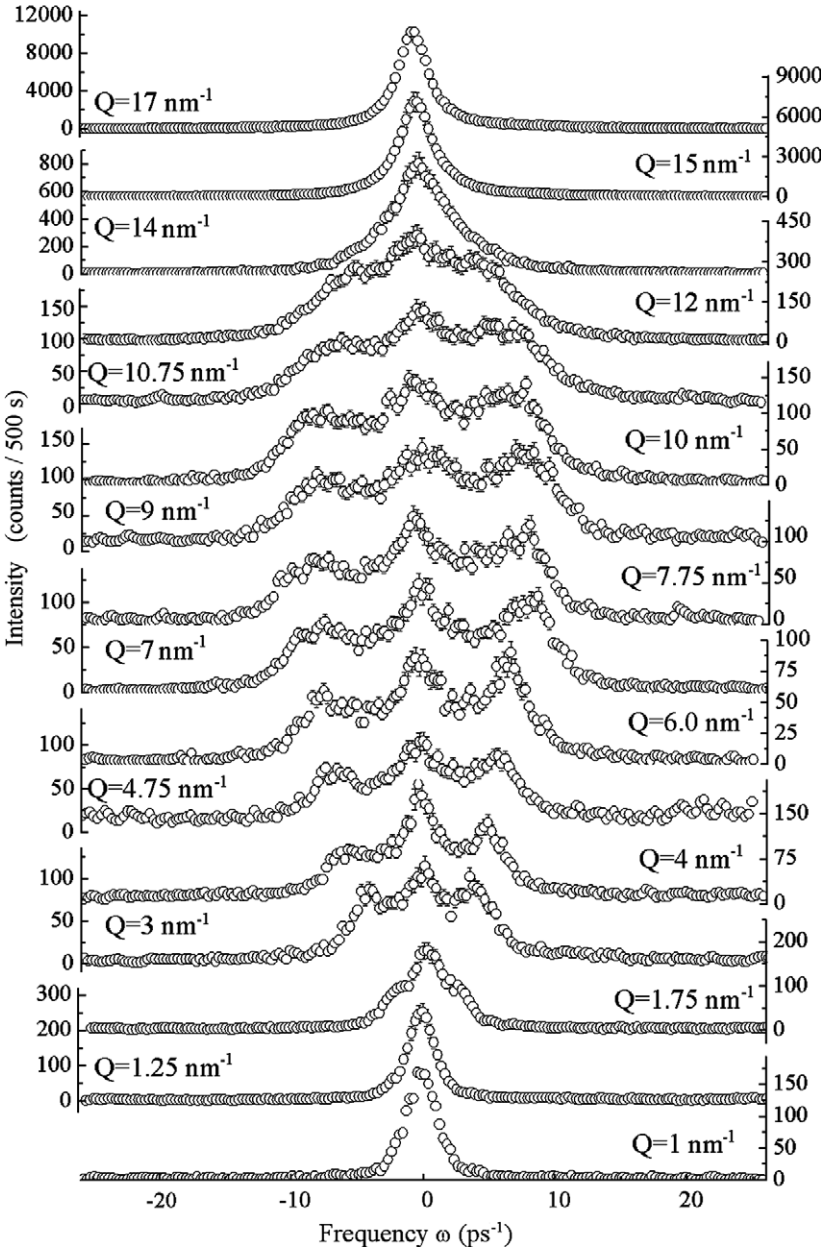

Fig. 1. IXS spectra of liquid potassium at $T = 343$ K and at the indicated Q values. The error bars are not reported when they are smaller than the size of the data symbols.

behavior, with distinct time scales (τ_α and τ_μ) to describe the viscous contribution to the spectral shape. The slower exponential decay (τ_α) is able to take into account the structural α relaxation, the faster one (τ_μ) instead describes a rapid vibrational decorrelation of the atomic dynamics at earlier times.

By means of a fitting procedure we focused our attention to ascertain the presence of these two viscous relaxation processes and their typical time scale. Then we choose as free parameters of the fit, the microscopic and the structural relaxation times with their respective relaxation strengths (i.e. τ_α, τ_μ, Δ_α, Δ_μ, while all the other parameters have been kept fixed. We report in Fig. 2, a comparison between the best fitting line shape and the experimental spectra. The intensity has been normalized using the $S(Q)$ value deduced directly from the spectra through the first spectra moments

$$I_N(Q,\omega) = S(Q)\frac{I(Q,\omega)}{\int I(Q,\omega)\mathrm{d}\omega},$$

$$S(Q) = \frac{\hbar Q^2}{2m}\left(\Omega_I^{(1)}/\Omega_I^{(0)} - \Omega_R^{(1)}/\Omega_R^{(0)}\right)^{-1}.$$

$\Omega_{I,R}^{(0,1)}$ are the first and zero moments of the resolution function (R) and spectra (I).

The central physical quantity characterizing the evolution of $S(Q,\omega)$ at different Q values is represented by ω_l, the frequency position of the maxima in the longitudinal

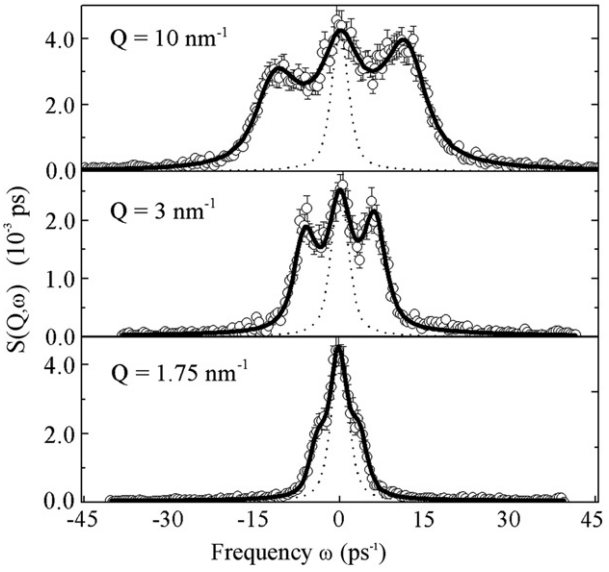

Fig. 2. Selected IXS experimental $S(Q,\omega)$ (open circles) are plotted with the respective fit functions (full line). The dotted line represents the resolution function (full-width at half height $\Delta E \approx 1.5$ meV).

current correlation spectra $J_l(Q,\omega) = (\omega^2/Q^2)S(Q,\omega)$. In Fig. 3 we plot ω_l vs Q with the data obtained from the INS [3,4], the three different measurements are in reasonable agreement with each other down to Q values close to 3 nm^{-1}. Moreover, the possibility offered by IXS to probe also the low Q region allows us to extend the study of the dynamics of the system where the transition from the isothermal ω_0 to the fully unrelaxed regime ω_∞ starts to be visible.

In order to investigate the microscopic origin of the ω_l dispersion we look directly to the apparent speed of sound (Fig. 3) and we compare the different relaxation contributions with the two speeds of sound limits: the generalized isothermal value c_t (limit in the low Q region) and the high frequency limit c_∞. For this last quantity we use the value estimated by the structural data following the formula [11,12]

$$c_\infty(Q) = \sqrt{\frac{3K_BT}{m} + \frac{\rho}{mQ^2}\int \frac{\partial^2 V(r)}{\partial z^2}(1 - e^{-iQz})g(r)d^3r}.$$

The value of $g(r)$ involved in the formula of c_∞, has been estimated by a molecular dynamic simulation using a Price–Singwi–Tosi pseudo-potential [21].

The increase of the apparent speed of sound between $1 < Q < 3$ nm^{-1} in Fig. 3 represents a characteristic shared with many other simple fluids, that is commonly rationalized as the signature of a transition between a liquid like to a solid like process. More specifically, the INS studies recognize the similarity of the high frequency sound velocity values with the acoustic phonons excitation of the crystal, as a supporting evidence of this interpretation.

The recourse to generalized hydrodynamics with two distinct viscous relaxation processes, however, allows inferring about this explanation of the positive dispersion in the liquid.

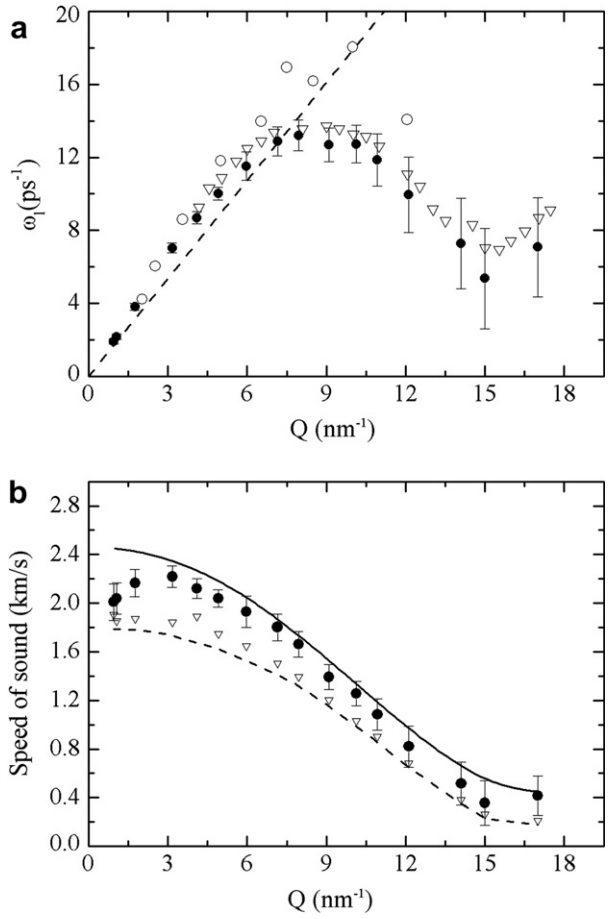

Fig. 3. (a) The full dots are the ω_l value obtained from the fits of IXS data, the results of recent INS studies are reported with open symbols (open triangle [2] end open circle [3]). The dashed line indicates the hydrodynamic isothermal limit. (b) The sound velocities deduced from IXS measurements are shown: ω_l/Q (full circle), $c_0(Q)$ (dashed line). The full line represents the $c_\infty(Q)$ calculated from structural data, the empty triangles are the unrelaxed sound velocity of the structural relaxation process $c_\alpha(Q)$.

In Fig. 3, we report the Q dependence of the sound velocity and the contribution to its value arising from the structure relaxation process: $c_\alpha = (\omega_0^2 + \Delta_\alpha^2)^{1/2}/Q$ – i.e. the velocity which is reached if the structural relaxation is fully unrelaxed ($\omega\tau_\alpha \gg 1$). When all relaxation processes are frozen, the speed of sound has the limiting value of $c_\infty = (\omega_0^2 + \Delta_\alpha^2 + \Delta_\mu^2)^{1/2}/Q$. Clearly, from Fig. 3, c_α does not account for the whole positive dispersion effect: $c_l(Q_m) = 2240$ m/s at $Q = 3$ nm^{-1} is higher of the isothermal low Q limit value of 1790 m/s. This behavior than the sound velocity, exceeding c_α all over the probed Q range indicates that the dynamics of the system, though above the melting point, appears solid like in the whole probed frequency region (i.e. $\omega\tau_\alpha \gg 1$). The magnitude of c_α relative to c_∞, however, is always rather small (10%). As consequence of this observation, we can attribute the transition from c_0 to c_∞ to the relaxation of the

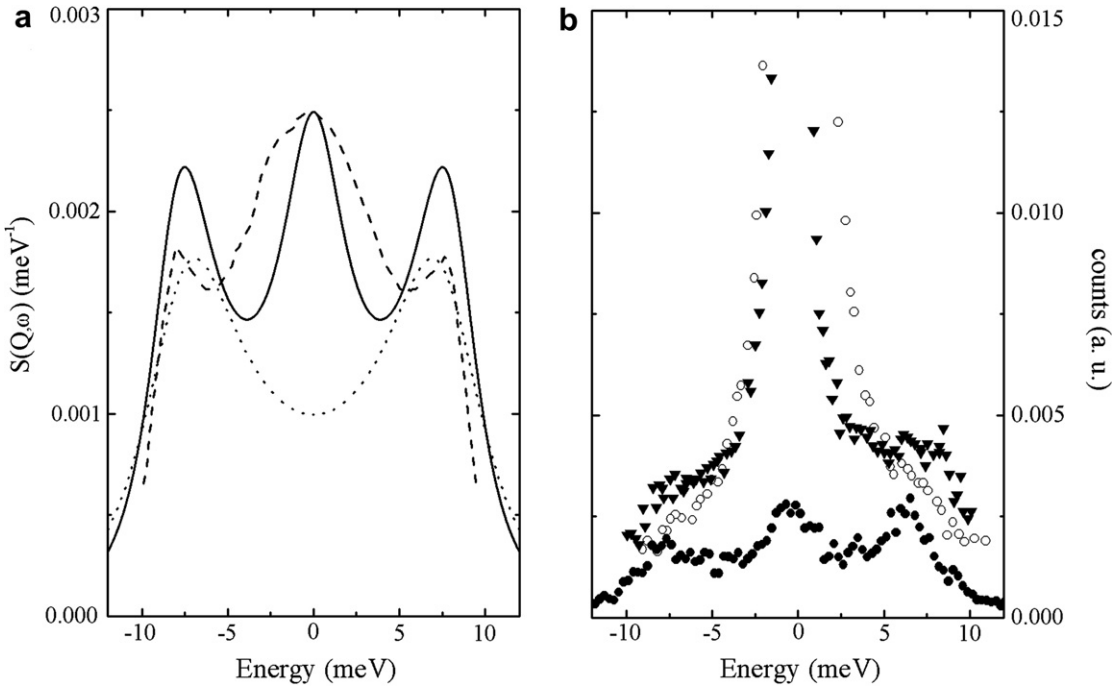

Fig. 4. (a) The full line shows the $S(Q,\omega)$ value at $Q = 6\ \mathrm{nm}^{-1}$ obtained from the best fit results of the IXS spectra. The data are deconvolved from the experimental resolution. The dashed line is the coherent signal at $6\ \mathrm{nm}^{-1}$ of the INS measurement [2], the dotted line represents the DHO contributed at $6.5\ \mathrm{nm}^{-1}$ to the coherent signal of the most recent measurement of INS [3]. (b) The raw IXS spectra (full dots) are compared with the INS data (open circle [3], full triangle [2]). All data are normalized to the same integral value of the coherent signal.

microscopic process still active in the low Q region and independent by the diffusional motion of the system. Passing from 1 to $3\ \mathrm{nm}^{-1}$, the microscopic process progressively relaxes (i.e. $\omega_l\tau_\mu(Q=1) \approx 0.25$ increases up to $\omega_l\tau_\mu(Q=3) \approx 0.75$) while the structural relaxation process is already relaxed ($\omega_l\tau_\alpha \approx 6$ in the all probed Q range). The positive dispersion effect, therefore, can be regarded as driven by the disorder of the inherent structure underlying the liquid dynamics, rather than by a liquid to solid like dynamical transition of the system. This last effect, although present, does not occur in the accessible experimental window and it is quantitatively negligible.

The relaxation scenario depicted so far has also significant implications on the lineshape behavior of $S(Q,\omega)$ and, therefore, a direct comparison with the lineshapes measured with neutron scattering technique can be extremely helpful.

In Fig. 4, we show that the coherent signal extracted from both the INS measurements [3,4] indivate a position for the maxima of the inelastic features (and therefore of the sound velocity) compatible with that deduced from IXS data. A spectral comparison over the whole energy range, however, reveals significant differences. The analysis of Bermejo et al. [3], having chosen as a starting model a viscoelastic approximation (though going one step further into the closure level of the memory functions hierarchy) naturally accounts for a quasielastic coherent component. Thus, the whole lineshape is in a rather good agreement with the independent X-ray measurements, despite the additional effect as: differences in instrumental resolution shapes, multiple scattering and phonon contribution. The analysis of Bove et al. [4], on the other hand, is based on a DHO model and Fig. 4 shows how this empirical model can work fairly well for the purpose to estimate the position of the maxima of the coherent $S(Q,\omega)$. However on the basis of this comparison it emerges that the determination of the coherent dynamic structure factor is heavily affected by the way to account for the quasielastic incoherent signal. The need to include a quasielastic component to describe the collective dynamics of the liquid clearly appears.

4. Conclusion

In conclusion, we presented in this paper an inelastic X-ray study of liquid potassium near the melting point, covering a quite large Q region from $1\ \mathrm{nm}^{-1}$ up to $16\ \mathrm{nm}^{-1}$. Thanks to the quality of the collected data, we have been able to follow the positive dispersion phenomenology over a wide energy range in the low Q region undisclosed by previous INS measurements. In order to gather detailed information on the microscopic nature of the dynamics of the system, we tested the reliability of a model characterized by the presence of three different channels for the decay of the density fluctuations.

This approach allows probing the physical processes underlying the relaxation dynamics, exploiting the information coming from the whole lineshape of our spectra.

In particular, the presence of two distinct viscous relaxation processes gives us a robust argument to attribute the behavior of the acoustic properties of the liquid to a relaxation process with a sub-pico-second time scale τ_μ. Such time scale is much faster for the characteristic structural relaxation time of the system τ_α. Thus, the anomalous behavior of sound velocity can be attributed to the interaction of the sound mode with the 'instantaneous' disordered structure of the liquid, since in the observed time scale the atoms have well defined equilibrium position ($\omega\tau_\alpha \gg 1$). This interpretation, is also supported by the results obtained in numerical simulation of Lennard–Jones system [22].

Finally, a comparison of the spectra achieved with neutrons and X-rays measurements shows how the recent refinement of the INS instruments/data analysis now allows the extraction of reliable information on the sound dispersion properties. On the other hand, any conclusions about the ultimate nature of the acoustic properties are highly dependent from the whole lineshape of the coherent signal and, therefore, an independent reliable description of the incoherent neutron scattering is necessary for an accurate description of collective properties. In this respect, a combined application of the two techniques (the IXS data might be used as input to subtract the coherent contribution from INS spectra), could allow for an absolute determination of the incoherent scattering in those systems with significant coherent neutron scattering cross section.

Acknowledgements

We kindly thank C. Cabrillo for a fruitful email exchange and L.E. Bove for useful discussions.

References

[1] T. Scopigno, G. Rocco, F. Sette, Rev. Mod. Phys. 77 (2005) 881.
[2] A.G. Novikov, V.V. Savostin, A.L. Shimkevich, R.M. Yulmetyev, Physica B 228 (1996) 312.
[3] C. Cabrillo, F.J. Bermejo, M. Alvarez, P. Verkerk, A. Maira-Vidal, S.M. Bennington, D. Martín, Phys. Rev. Lett. 89 (2002) 075508.
[4] L. Bove, B. Dorner, C. Petrillo, F. Sacchetti, J. Suck, Phys. Rev. B 68 (2003) 024208.
[5] T. Scopigno, A. Filipponi, M. Krisch, G. Monaco, G. Ruocco, F. Sette, Phys. Rev. Lett. 89 (2002) 255506.
[6] T. Scopigno, U. Balucani, G. Ruocco, F. Sette, Phys. Rev. E 65 (2002) 031205.
[7] H. Sinn et al., Phys. Rev. Lett. 78 (1997) 1715.
[8] W.C. Pilgrim, S. Hosokawa, H. Saggau, H. Sinn, E. Burkel, J. Non-Cryst. Solids 96 (1999) 250.
[9] T. Scopigno, U. Balucani, G. Ruocco, F. Sette, Phys. Rev. Lett. 85 (2000) 4076.
[10] T. Scopigno, U. Balucani, G. Ruocco, F. Sette, Phys. Rev. E 63 (2001) 011210.
[11] U. Balucani, M. Zoppi, Dynamics of the Liquid State, Clarendon, Oxford, 1983.
[12] J.P. Boon, S. Yip, Molecular Hydrodynamics, McGraw-Hill, NY, 1980.
[13] A. Rahman, Phys. Rev. Lett. 32 (1974) 52.
[14] U. Balucani, A. Torcini, R. Vallauri, Phys. Rev. A 46 (1992) 2159.
[15] S. Kambayashi, G. Kahl, Phys. Rev. A 46 (1992) 3255.
[16] F. Shimojo, K. Hoshino, M. Watabe, J. Phys. Soc. Jpn. 63 (1994) 141.
[17] T. Scopigno, G. Ruocco, F. Sette, G. Viliani, Phys. Rev. E 66 (2002) 031205.
[18] T. Scopigno, U. Balucani, G. Ruocco, F. Sette, Phys. Rev. E 63 (2001) 011210.
[19] W. Ohse et al., Handbook of Thermodynamic and Transport Properties of Alkali Metals, Blackwell Scientific, Oxford, 1985.
[20] J.R.D. Copley, S.W. Lovesey, Rep. Prog. Phys. 38 (1975) 461.
[21] D.L. Price, K.S. Singwi, M.P. Tosi, Phys. Rev. B 2 (1970) 2983.
[22] G. Ruocco, F. Sette, R. Di Leonardo, G. Monaco, M. Sampoli, G. Viliani, Phys. Rev. Lett. 84 (2000) 5788.